

# The GLD-2 poly(A) polymerase activates *gld-1* mRNA in the *Caenorhabditis elegans* germ line

Nayoung Suh\*, Britta Jedamzik†, Christian R. Eckmann†, Marvin Wickens\*, and Judith Kimble\*<sup>‡§</sup>

\*Department of Biochemistry and †Howard Hughes Medical Institute, University of Wisconsin, 433 Babcock Drive, Madison, WI 53706-1544; and ‡Max Planck Institute of Molecular Cell Biology and Genetics, Pfotenhauerstrasse 108, 01307 Dresden, Germany

Contributed by Judith Kimble, August 15, 2006

mRNA regulation is crucial for many aspects of metazoan development and physiology, including regulation of stem cells and synaptic plasticity. In the nematode germ line, RNA regulators control stem cell maintenance, the sperm/oocyte decision, and progression through meiosis. Of particular importance to this work are three GLD (germ-line development) regulatory proteins, each of which promotes entry into the meiotic cell cycle: GLD-1 is a STAR/Quaking translational repressor, GLD-2 is a cytoplasmic poly(A) polymerase, and GLD-3 is a homolog of Bicaudal-C. Here we report that the *gld-1* mRNA is a direct target of the GLD-2 poly(A) polymerase: polyadenylation of *gld-1* mRNA depends on GLD-2, the abundance of GLD-1 protein is dependent on GLD-2, and the *gld-1* mRNA coimmunoprecipitates with both GLD-2 and GLD-3 proteins. We suggest that the GLD-2 poly(A) polymerase enhances entry into the meiotic cell cycle at least in part by activating GLD-1 expression. The importance of this conclusion is twofold. First, the activation of *gld-1* mRNA by GLD-2 identifies a positive regulatory step that reinforces the decision to enter the meiotic cell cycle. Second, *gld-1* mRNA is initially repressed by FBF (for *fem-3* binding factor) to maintain stem cells but then becomes activated by the GLD-2 poly(A) polymerase once stem cells begin to make the transition into the meiotic cell cycle. Therefore, a molecular switch regulates *gld-1* mRNA activity to accomplish the transition from mitosis to meiosis.

cytoplasmic poly(A) polymerase | RNA regulation | mitosis/meiosis decision

Expression of mRNA is tightly regulated during metazoan development (1). One common mechanism of mRNA control relies on regulated polyadenylation. In the nucleus, poly(A) tails are added by a poly(A) polymerase (PAP) that acts on virtually all RNA polymerase II transcripts (2). However, in the cytoplasm, poly(A) tails are maintained or lengthened by a cytoplasmic PAP (cPAP) that acts specifically on a subset of mRNAs (3). These cPAPs, known as GLD-2 in metazoans (4), were discovered in *Caenorhabditis elegans* and *Schizosaccharomyces pombe* (4–6). A common biological function of GLD-2 has been inferred from null mutants in *C. elegans* (7) and molecular experiments in *Xenopus* (8, 9). In both cases, GLD-2 controls germ-line progression through meiosis. Furthermore, in *C. elegans*, GLD-2 controls the decision between mitosis and meiosis (7). In this work, we identify a direct target of GLD-2 in *C. elegans*.

The mitosis/meiosis decision in *C. elegans* is controlled by Notch signaling and four broadly conserved RNA regulatory proteins (Fig. 1). Notch signaling and FBF (for *fem-3* binding factor) are both required for maintenance of germ-line stem cells (10). FBF is an RNA-binding protein of the PUF (for Pumilio and FBF) family (11). Notch signaling activates transcription of the *fbf-2* gene (12), and FBF represses *gld-1* and *gld-3* mRNAs (Fig. 1). Three *gld* genes (for germ-line development) promote entry into the meiotic cell cycle (7, 13). GLD-1 is a STAR RNA-binding protein and translational repressor (14, 15); GLD-2 is the catalytic subunit of a cPAP (4); and GLD-3 is a Bicaudal-C homolog that possesses five KH motifs and is predicted to bind RNA (4, 16). Like other cPAPs, nematode GLD-2

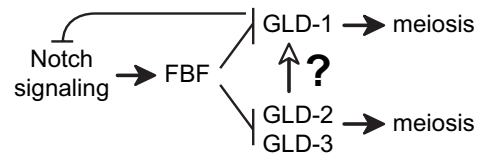


Fig. 1. Regulatory circuit controlling the mitosis/meiosis decision. Both Notch signaling and FBF promote mitotic cell divisions, whereas the GLD proteins promote entry into the meiotic cell cycle. FBF negatively regulates both *gld-1* and *gld-3* mRNAs. GLD-1 and GLD-2/GLD-3 represent parallel branches of the regulatory circuit, because each can promote entry into meiosis in the absence of the other. This work tests the hypothesis that the *gld-1* mRNA may be a direct target of the GLD-2 PAP (see text for details).

does not possess a recognizable RNA-binding domain (4). Instead, GLD-2 binds GLD-3, which stimulates its enzymatic activity *in vitro* (4). The GLD-2 and GLD-3 proteins appear to function together to promote entry into meiosis.

A key step in understanding how GLD-2 cPAP controls mRNAs is the identification of its direct targets. In this work, we present molecular data to demonstrate that the *gld-1* mRNA is a direct target of GLD-2 cPAP. Consistent with our findings, genetic data suggest that *gld-1* expression is controlled redundantly by GLD-2 and NOS-3 (17), which is a Nanos homolog (18). Identification of the *gld-1* transcript as a direct GLD-2 target defines a mechanism for positive reinforcement in the circuitry controlling the mitosis/meiosis decision and suggests an attractive model for a regulatory switch from mitosis- to meiosis-promoting activity.

## Results

**GLD-2 Regulates *gld-1* Poly(A) Tail Length.** To identify target mRNAs of the GLD-2 PAP, we used a candidate gene approach. The *gld-1* mRNA was a plausible candidate, because *gld-1* and *gld-2* both promote entry into meiosis (7). We first asked whether polyadenylation of *gld-1* mRNA is dependent on GLD-2. Specifically, we compared the lengths of poly(A) tails on endogenous *gld-1* mRNAs in wild-type animals and *gld-2* null mutants by using a “circularization RT-PCR” (cRT-PCR) assay (Fig. 2A) (19). Total RNA was prepared from wild-type and *gld-2(0)* mutants and then decapped and ligated to generate circular RNAs. RT-PCR of these circular RNAs was then performed by using primers that flank the poly(A) tail: one primer was specific to sequences near the 3' end of the mRNA of interest and the other primer was complementary to the trans-spliced leader present at the 5' end of many *C. elegans* mRNAs (20). Poly(A)

Author contributions: N.S., C.R.E., M.W., and J.K. designed research; N.S. and B.J. performed research; N.S. analyzed data; and N.S., C.R.E., M.W., and J.K. wrote the paper.

The authors declare no conflict of interest.

Abbreviations: GLD, germ-line development; FBF, *fem-3* binding factor; PAP, poly(A) polymerase; cPAP, cytoplasmic PAP; IP, immunoprecipitate; cRT-PCR, circularization RT-PCR; L4, fourth larval stage.

<sup>§</sup>To whom correspondence should be addressed. E-mail: jekimble@wisc.edu.

© 2006 by The National Academy of Sciences of the USA



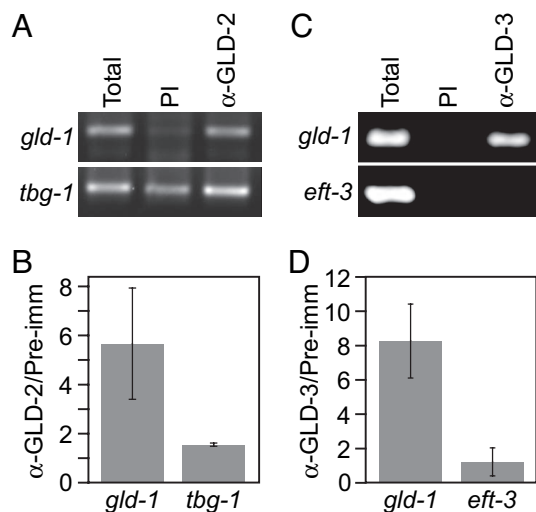


**Fig. 4.** GLD-2 and GLD-3 are physically associated with *gld-1* mRNA. (A) Coimmunoprecipitation of *gld-1* mRNA using GLD-2 antibody but not with preimmune serum (PI). (B) Real-time PCR analysis of *gld-1* and *tbg-1* mRNAs. (C) Coimmunoprecipitation of *gld-1* mRNA using GLD-3 antibody but not with preimmune serum (PI). (D) Real-time PCR analysis of *gld-1* and *eft-3* mRNAs.

cytochemistry (data not shown). We conclude that unlike GLD-2, GLD-3 is not crucial for activating *gld-1* expression.

***gld-1* mRNA Is Associated with GLD-2/GLD-3 PAP.** We next asked whether the GLD-2 and GLD-3 proteins interact physically with *gld-1* mRNA *in vivo*. Specifically, we incubated extracts that had been prepared from wild-type animals with GLD-2-specific or GLD-3-specific antibodies, isolated the immunoprecipitate (IP), and used both RT-PCR and quantitative real-time PCR to assess the presence of *gld-1* and control mRNAs (Fig. 4). By RT-PCR, *gld-1* mRNA was enriched in the GLD-2 IP compared with a precipitate with preimmune serum (PI), whereas *tbg-1* mRNA was present in both preimmune and GLD-2 IPs (Fig. 4A). By real-time PCR, *gld-1* mRNA was enriched  $\approx 6$ -fold in the anti-GLD-2 IP versus preimmune serum (Fig. 4B; range 3- to 8-fold in multiple experiments); *tbg-1* mRNA was not enriched (Fig. 4B). The simplest explanation is that *gld-1* mRNA associates specifically with GLD-2 protein in worm extracts.

*gld-1* mRNA was also enriched in IPs with GLD-3 antibody compared with preimmune serum. The negative control *eft-3* mRNA was not detected in GLD-3 IP (Fig. 4C). *eft-3* encodes a translation elongation factor 1 $\alpha$  that is expressed in the germ line (23). By real-time PCR, *gld-1* mRNA was enriched  $\approx 8$ -fold in the anti-GLD-3 IP versus preimmune serum (Fig. 4D; range 6- to 10-fold in multiple experiments); *eft-3* mRNA was not enriched (Fig. 4D). We conclude that *gld-1* mRNA associates specifically with GLD-3 protein in worm extracts.

## Discussion

**GLD-2 PAP Activates Expression of its Target mRNA.** We have identified *gld-1* mRNA as a direct target of the GLD-2 PAP. Importantly, GLD-2 activates *gld-1* expression. In *gld-2* null mutants, both *gld-1* mRNA and GLD-1 protein are less abundant than in wild-type animals. We cannot exclude the formal possibility that GLD-2 controls *gld-1* transcription. However, GLD-2 is a cytoplasmic protein with PAP activity (4), and its *Xenopus* counterpart regulates cytoplasmic mRNAs (8, 9). Therefore, a more likely interpretation is that GLD-2 controls RNA stability and perhaps translation.

Both *gld-1* mRNA and GLD-1 protein are reduced in *gld-2* mutants, but the reduction is more severe for the mRNA than

for the protein (9-fold versus 2.5-fold). This difference can be explained in various ways. The simplest explanation is that levels of mRNA and protein may be differentially subject to indirect effects of GLD-2 loss. For example, the GLD-1 protein, but not the RNA, may be stabilized in *gld-2* mutants because of effects on some other regulator. A more intriguing idea is that GLD-2 is involved in translational repression in addition to its effect on mRNA stability. By this scenario, the less abundant *gld-1* mRNA would be translationally more active in *gld-2* mutants.

The ability of GLD-2 to activate expression of target mRNAs is similar to findings for its closely related *Xenopus* homolog: XI-GLD-2 activates expression of cyclin B mRNA (8, 9). By contrast, the more distant homolog in *Saccharomyces cerevisiae*, known as TRF4, polyadenylates selected RNAs in the nucleus and targets them for destruction (24). We suggest that metazoan GLD-2 PAPs activate expression of their target mRNAs in the cytoplasm.

***gld-1* Activation by GLD-2 Reinforces Decision to Enter Meiosis.** Entry into meiosis is controlled by two redundant pathways, which together provide the major control for the transition from mitosis to meiosis (7) (Fig. 1). In one branch is the GLD-1 translational repressor, which likely promotes entry into meiosis by down-regulating mRNAs required for mitosis. In the other branch is the GLD-2 translational activator, which likely promotes entry into meiosis by activating mRNAs required for meiosis. Also in the second branch is GLD-3, which appears to act with GLD-2 to generate a heterodimeric PAP (4, 13) (see below).

In single mutants lacking *gld-1*, *gld-2*, or *gld-3*, germ cells are capable of entering meiosis, although entry does not occur normally (7). Indeed, the switch from mitosis to meiosis appears to be delayed in *gld-2* and *gld-3* null mutants (13). A molecular understanding of the switch requires identification of direct targets of both the GLD-1 repressor and GLD-2 activator. Numerous direct targets of GLD-1 translational repression are known, but none to date control the mitosis/meiosis decision (15, 25). This work identifies *gld-1* mRNA as a direct target of the GLD-2 activator. However, *gld-1* mRNA cannot be the only GLD-2 target, because GLD-2 is able to promote entry into meiosis in the absence of GLD-1. Instead, we suggest that *gld-1* activation by GLD-2 strengthens the switch from mitosis to meiosis, an idea that is consistent with the switch delay in *gld-2* null mutants.

**Do GLD-2 and GLD-3 Work Together to Activate *gld-1* mRNA?** A remaining question is whether GLD-3 functions together with GLD-2 to polyadenylate *gld-1* mRNA. Several lines of evidence support that idea. First, *gld-2* and *gld-3* null mutants are similar with respect to their effects on the decision between mitosis and meiosis. In *gld-2* and *gld-3* single mutants, the mitotic region is enlarged to an equivalent extent, suggesting that the two proteins play a similar role in the transition into meiosis (13). As double mutants with *gld-1*, they also have similar effects: both *gld-1 gld-2* and *gld-1 gld-3* double mutants have tumorous germ lines (7, 13). Second, the GLD-2 and GLD-3 proteins coimmunoprecipitate from worm extracts and therefore appear to be physically associated *in vivo* (13). Third, GLD-3 enhances GLD-2 enzymatic activity *in vitro* (4). These results, when taken together, support the model that GLD-2 and GLD-3 work together as a heterodimeric enzyme to promote meiosis. Consistent with that idea, *gld-1* mRNA immunoprecipitates with antibodies specific to either GLD-2 or GLD-3 (this work). The simplest explanation is that GLD-2 and GLD-3 function together to polyadenylate the *gld-1* transcript.

Although GLD-2 and GLD-3 are likely to work together to control entry into meiosis, they do not have equivalent roles in

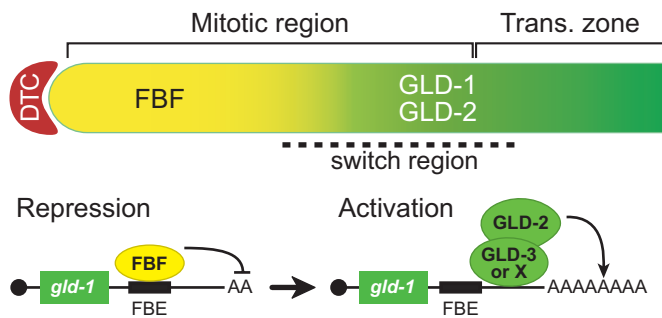


**Fig. 5.** Model for molecular switch controlling *gld-1* mRNA. (Upper) Diagram of distal germ line. DTC is the somatic distal tip cell that provides the niche for germ-line stem cells; the mitotic region spans the extent of any mitotically dividing germ cells; the transition zone includes nuclei in early stages of meiotic prophase; and the switch region contains nuclei transitioning from mitotic to meiotic cell cycle. Solid yellow, FBF promotes continued mitotic divisions; solid green, GLD proteins promote meiosis; gradient from yellow to green, transition from mitosis to meiosis. (Lower) FBF repression of *gld-1* mRNA (Left), and GLD-2 activation of same mRNA (Right). FBE, FBF-binding element in the *gld-1* 3' untranslated region. Figure is not to scale.

*gld-1* mRNA activation. Whereas GLD-1 levels decreased in *gld-2* null mutants, they remained normal in *gld-3* null mutants. Molecular redundancy appears to be the rule in the circuitry controlling the mitosis/meiosis decision (7, 12). Moreover, GLD-2 binds additional RNA-binding proteins whose functions are not yet known (L. Wang and J.K., unpublished data). We suggest that GLD-2 can accomplish *gld-1* polyadenylation with either GLD-3 or another RNA-binding protein (Protein X in Fig. 5 Lower) that remains unknown.

#### Dual Control of *gld-1* mRNA Suggests Existence of a Molecular Switch.

The identification of *gld-1* mRNA as a direct target of the GLD-2 PAP is of particular interest because *gld-1* mRNA is also a direct target of repression by the PUF protein FBF (26). Fig. 5 presents a simple model for this dual control of *gld-1* mRNA as germ cells move from the niche provided by the distal tip cell and progress proximally. As germ cells escape Notch signaling and FBF repression, they leave the mitotic cell cycle and enter meiosis. FBF promotes continued mitotic divisions, in part by repressing *gld-1* mRNA (26). GLD-2 promotes entry into meiosis, in part by activating the same mRNA. The mechanism by which *gld-1* mRNAs switch from FBF-dominated repression to a GLD-2-dominated activation is currently unknown.

One attractive possibility is that FBF and GLD-2 are components of a molecular switch. By this scenario, FBF would repress mRNAs in cells within the stem cell niche, which lack GLD-2, but FBF might also mark those same mRNAs for activation once cells had left the niche and GLD-2 became available. Consistent with that idea, FBF, which is encoded by two nearly identical genes, *fbf-1* and *fbf-2* (11), acts genetically in the GLD-2/GLD-3 branch of control: the germ line of *gld-1; fbf-1 fbf-2* triple mutants is tumorous (26), an effect similar to that seen in *gld-1; gld-2* and *gld-1; gld-3* double mutants (7, 13). Regardless, we conclude that the GLD-2 PAP activates the same mRNA that FBF represses and that both controls are critical for the germ-line switch from mitosis to meiosis.

#### Methods

**Nematode Strains and Methods.** All strains were maintained at 20°C as described (27). Strains included wild-type *C. elegans* (N2) as well as *gld-2(q497)*, which is a nonsense mutation and putative null (4), and *gld-3(q730)*, which is a deletion mutation and

putative null (16). *gld-2(q497)* was balanced with *hT2[qIs48]*; *gld-3(q730)* was balanced with *mIn1[mIs14 dpy-10(e128)]*.

**cRT-PCR.** Total RNA from a mid-L4-staged population of animals was isolated by using TRIzol (Invitrogen, Carlsbad, CA). *gld-2(q497)* null animals were collected with a COPAS Biosort (Union Biometrica, Somerville, MA) from a population of *gld-2(q497)/hT2[qIs48]* animals, as described by the manufacturer. cRT-PCR was performed as described in ref. 19 with a minor modification: 4 μg of total RNA was used for the oligo(dT)/RNase H treatment, decapping, and circularization steps. SL1 reverse primer (SL1r) or SL2 reverse primer (SL2r) were used for reverse-transcriptase reaction with SuperScript III reverse transcriptase (Invitrogen). Nested PCRs were performed and analyzed by using 5% Criterion TBE gels (Bio-Rad, Hercules, CA). Five independent clones were obtained from each experiment and sequenced. The primer sequences are available from the authors upon request.

**Western Blots and Immunocytochemistry.** Whole worm lysates prepared from mid- to late-L4 hermaphrodites were analyzed by both immunoblotting and immunohistochemistry. Anti-GLD-1 antibodies were used at a 1:750 dilution in Western blot analysis and at a 1:100 dilution in immunohistochemistry. Gonad dissections (28) and Western blots (29) were performed as described. The anti-α-tubulin antibody (Sigma, St. Louis, MO) was diluted 1:20,000, and Mab-414 (Berkeley Antibody, Richmond, CA) was diluted 1:400. Cy-3-labeled donkey anti-rabbit and FITC-labeled donkey anti-mouse (Jackson Laboratories, Bar Harbor, ME) were used as secondary antibodies (dilution 1:500) in immunohistochemistry. AP-conjugated donkey anti-rabbit (Pierce, Rockford, IL) and HRP-conjugated donkey anti-mouse (Jackson Laboratories) antibodies were used for Western blots (dilution 1:40,000). Confocal images were obtained on a Bio-Rad MRC1024 confocal microscope. Fluorescence was quantified by using National Institutes of Health ImageJ software as described (12).

**Immunoprecipitations.** N2 worms were grown on standard NGM agar plates and collected by centrifugation, then washed several times in M9 buffer, with final wash in PBS with 1 μl/ml RNaseOUT (Invitrogen) and an EDTA-free protease inhibitor mixture (Roche, Indianapolis, IN). Crude extract was then prepared by lysing the animals by using a French press at 19,000 psi two times. Samples were then centrifuged at 200 × g before being stored at −80°C and again at 16,000 × g immediately before use. Trisacryl-immobilized protein-A beads (Pierce) bound to anti-GLD-2 (rabbit α-GLD-2) (4) or preimmune controls were equilibrated with PBS and incubated overnight at 4°C with 500-μg extracts for each immunoprecipitation. Beads were subsequently washed five times with 0.5 ml of PBS. RNA was eluted from beads by extraction with TRIzol (Invitrogen) and solubilized in 20 μl of diethylpyrocarbonate water. Anti-GLD-3 (rb156) (16) or preimmune antibodies were first incubated for 1 h at 4°C with extracts supplemented with 1% Nonidet P-40 and subsequently captured on protein-A beads (Roche) for another hour before washing beads five times in 1× PBS/1% Nonidet P-40.

**RT-PCR and Quantitative Real-Time PCR.** Reverse-transcriptase reactions were performed by using cDNA cloning primer (Integrated DNA Technologies, Inc., Coralville, IA) and SuperScript III reverse transcriptase (Invitrogen) with all coimmunoprecipitated samples or 5 μg of total input RNA. The reverse-transcription reaction (1 μl) was used for PCR with gene-specific primers for 30 cycles with an annealing temperature of 57°C (*gld-1*) and 53°C (*tbg-1*). RT-PCR products (40%) were analyzed with 2% agarose gel. We used

real-time RT-PCR to quantify the mRNA enrichment in immunoprecipitated samples. Real-time RT-PCR was performed in 40 cycles of 95°C for 15 s and 60°C for 1 min by using the SmartCycler System (Cepheid, Sunnyvale, CA). The set of primers for each gene preferentially span an intron and sizes range from 100 to 150 bp, and gene-specific fluorogenic probes were obtained from Integrated DNA Technologies. The Taq-Man Universal PCR Master Mix (Applied Biosystems, Foster City, CA) was used according to the manufacturer's guidelines.

The primer and probe sequences are available from the authors upon request.

We thank members of the J.K. and M.W. laboratories for comments on the manuscript, J. W. Pike for advice on using the Cepheid SmartCycler System, and E. B. Goodwin for the GLD-1 antibody. J.K. and M.W. are supported by the National Institutes of Health; J.K. is an Investigator of the Howard Hughes Medical Institute. C.R.E. is supported by the Max Planck Society.

1. Thompson B, Wickens M, Kimble J (2007) in *Translational Control in Biology and Medicine*, eds Mathews MB, Sonenberg N, Hershey JWB (Cold Spring Harbor Lab Press, Woodbury, NY), in press.
2. Edmonds M (2002) *Prog Nucleic Acid Res Mol Biol* 71:285–389.
3. Richter JD (2000) in *Translational Control of Gene Expression*, eds Sonenberg N, Hershey JWB, Mathews MB (Cold Spring Harbor Lab Press, Woodbury, NY), pp 785–805.
4. Wang L, Eckmann CR, Kadyk LC, Wickens M, Kimble J (2002) *Nature* 419:312–316.
5. Read RL, Martinho RG, Wang S-W, Carr AM, Norbury CJ (2002) *Proc Natl Acad Sci USA* 99:12079–12084.
6. Saitoh S, Chabes A, McDonald WH, Thelander L, Yates JR, III, Russell P (2002) *Cell* 109:563–573.
7. Kadyk LC, Kimble J (1998) *Development (Cambridge, UK)* 125:1803–1813.
8. Barnard DC, Ryan K, Manley JL, Richter JD (2004) *Cell* 119:641–651.
9. Rouhana L, Wang L, Buter N, Kwak JE, Schiltz CA, Gonzalez T, Kelley AE, Landry CF, Wickens M (2005) *RNA* 11:1117–1130.
10. Kimble J, Crittenden SL (August 15, 2005) *WormBook*, 10.1895/wormbook.1.13.1, www.wormbook.org.
11. Zhang B, Gallegos M, Puoti A, Durkin E, Fields S, Kimble J, Wickens MP (1997) *Nature* 390:477–484.
12. Lamont LB, Crittenden SL, Bernstein D, Wickens M, Kimble J (2004) *Dev Cell* 7:697–707.
13. Eckmann CR, Crittenden SL, Suh N, Kimble J (2004) *Genetics* 168:147–160.
14. Jones AR, Francis R, Schedl T (1996) *Dev Biol* 180:165–183.
15. Jan E, Motzny CK, Graves LE, Goodwin EB (1999) *EMBO J* 18:258–269.
16. Eckmann CR, Kraemer B, Wickens M, Kimble J (2002) *Dev Cell* 3:697–710.
17. Hansen D, Wilson-Berry L, Dang T, Schedl T (2004) *Development (Cambridge, UK)* 131:93–104.
18. Kraemer B, Crittenden S, Gallegos M, Moulder G, Barstead R, Kimble J, Wickens M (1999) *Curr Biol* 9:1009–1018.
19. Couttet P, Fromont-Racine M, Steel D, Pictet R, Grange T (1997) *Proc Natl Acad Sci USA* 94:5628–5633.
20. Nilsen TW (1993) *Annu Rev Microbiol* 47:413–440.
21. Christensen S, Kodoyianni V, Bosenberg M, Friedman L, Kimble J (1996) *Development (Cambridge, UK)* 122:1373–1383.
22. Strome S, Powers J, Dunn M, Reese K, Malone CJ, White J, Seydoux G, Saxton W (2001) *Mol Biol Cell* 12:1751–1764.
23. Maciejowski J, Ahn JH, Cipriani PG, Killian DJ, Chaudhary AL, Lee JJ, Voutev R, Johnsen RC, Baillie DL, Gunsalus KC, et al. (2005) *Genetics* 169:1997–2011.
24. Anderson JT (2005) *Curr Biol* 15:R635–R638.
25. Lee M-H, Schedl T (2001) *Genes Dev* 15:2408–2420.
26. Crittenden SL, Bernstein DS, Bachorik JL, Thompson BE, Gallegos M, Petcherski AG, Moulder G, Barstead R, Wickens M, Kimble J (2002) *Nature* 417:660–663.
27. Brenner S (1974) *Genetics* 77:71–94.
28. Lee M-H, Hook B, Lamont LB, Wickens M, Kimble J (2006) *EMBO J* 25:88–96.
29. Harlow E, Lane D (1988) *Antibodies, A Laboratory Manual* (Cold Spring Harbor Lab Press, Woodbury, NY).